Available online at www.sciencedirect.com
SCIENCE DIRECT®
Journal of Nuclear Materials 345 (2005) 101–108
journal of nuclear materials
www.elsevier.com/locate/jnucmat

Hydrogen ion bombardment damage in stainless steel mirrors

A.I. Belyaeva [a], A.F. Bardamid [b], J.W. Davis [c], A.A. Haasz [c,*], V.G. Konovalov [d], A.D. Kudlenko [a], M. Poon [c], K.A. Slatin [a], V.S. Voitsenya [d]

[a] National Technical University 'KhPI', Kharkov, 61002 Kharkov, Ukraine
[b] T. Shevchenko National University, Kiev, Ukraine
[c] University of Toronto Institute for Aerospace Studies, Toronto, ON, Canada M3H 5T6
[d] NSC KIPT, 61108 Kharkov, Ukraine

Received 14 December 2004; accepted 19 April 2005

Abstract

Experiments have been performed to evaluate the changes in surface structure and the resulting effects on the optical properties of stainless steel due to hydrogen ion irradiation. Stainless steel (SS) is a standard material used for in-vessel components, including the first mirrors (FMs), in some current generation fusion devices. Optical microscopy, interferometry, scanning electron microscopy (SEM) and ellipsometry were used to characterize the surfaces. Results are presented for the bombardment of SS mirrors with H_3^+ ions having various fixed energies (0.3, 0.65, and 1.5 keV/H^+), with ion flux densities of $(0.5–2)\times10^{20}$ H^+/m^2s and fluences of $\sim2.2\times10^{24}$ H^+/m^2. Variation of the ion energy at a constant fluence had a considerable effect on the damage structure that forms on the SS mirror surfaces. Possible mechanisms for the ion energy effect on the surface are discussed and a model of the damaged surface layer is proposed.

PACS: 78.68.+m; 78.70.−g

1. Introduction

Optical methods are widely used for plasma diagnostics in fusion devices, providing data on plasma parameters derived from the electromagnetic radiation emitted from the plasma. Directional control and spatial resolution of such diagnostics would be greatly limited without the use of first mirrors (FMs) placed close to the plasma. However, in high temperature plasmas such in-vessel mirrors will be subjected to irradiation by X-rays, gamma rays, neutrons, and charge exchange atoms with a wide energy range. The irradiation will affect the properties of FMs via sputtering, accumulation of gases, creation of defects, etc. Therefore, the criteria for the selection of materials for FMs should be made not only on the basis of their optical properties, but also on the material's resistance to degradation through plasma exposure.

Our interest in stainless steel (SS) mirrors stems from their use in some current fusion devices (e.g., Tore Supra [1,2], Large Helical Device [3], T-10 [4]) and potential use in next-generation large fusion devices. In addition, this material is one of the most suitable for providing

* Corresponding author. Tel.: +1 416 667 7734; fax: +1 416 667 7925.
E-mail address: aahaasz@utias.utoronto.ca (A.A. Haasz).

0022-3115/$ - see front matter © 2005 Elsevier B.V. All rights reserved.
doi:10.1016/j.jnucmat.2005.04.066

experimental data for modeling the behavior of mirrors in a fusion reactor. For the laboratory ion beam experiments performed in our study, the H^+ ion energies (300–1500 eV/H^+), fluxes ($\sim 10^{20}$ H^+/m^2s) and fluences ($1–4 \times 10^{24}$ H^+/m^2) have been chosen to roughly correspond to the bombardment conditions experienced by mirrors located near the first wall of a tokamak fusion reactor.

In a previous paper [5] the authors reported on the effect of H^+ irradiation on the reflectance of stainless steel mirrors using ellipsometry. They found a significant decrease in the reflectance with increasing H^+ fluence, and the decrease was more pronounced for higher ion energies. This optical degradation was attributed to the development of surface structure change during irradiation. Subsequent studies (Balden et al. [6] and the present work) have been undertaken to further investigate the evolution of the surface structure on subsets of the specimens. Balden et al. [6] have observed a strong micro-relief and a strong variation of the erosion depth for different grains using scanning electron microscopy (SEM). They also studied the correlation between surface morphology and the orientation of single grains using electron back-scattering diffraction. Grains with nearly (1 1 1) surface orientation do not show significant in-grain micro-relief, although they have nearly the highest erosion yield. Small variations of the angle between the ion impact direction and low index surfaces lead to strong changes in the erosion yield and to the creation of different in-grain features; no correlation was seen between erosion yield and roughness.

The objective of the present study was to further investigate the evolution of surface structure – erosion depth and step heights at grain boundaries – due to H^+ irradiation, using interferometry. Further ellipsometry measurements were also performed to assist in the development of a physical model of the SS mirror surface layer modified by heat treatment and ion impact.

2. Experiment

All mirror specimens were polycrystalline SS (04Cr16Ni11Mo3Ti – similar to SS316). Prior to H_3^+ irradiation, all specimens were mechanically polished using diamond powder with gradually decreasing particle size, starting with ~3 μm, then ~1 μm, followed by 300–500 nm, and finally 10 nm. For each particle size, a layer not less than the previous powder size was removed. For these specimens no electro-polishing was done, because in one particular case where it was done, an inferior mirror quality was obtained. The specimens were 7×7 mm^2 in size, and on each specimen only one spot (~5 mm diameter) was exposed to the ion beam.

Hydrogen ion irradiation was performed at the University of Toronto using mass-analyzed H_3^+ ions at normal incidence having various fixed energies with ion flux densities of $(0.5–2) \times 10^{20}$ H^+/m^2s and fluences of $\sim 2.2 \times 10^{24}$ H^+/m^2. (In this paper the impacting H particles in the H_3^+ ions are designated as H^+ even though the H_3^+ is only singly charged.) Each specimen was exposed to a different energy: 0.3 keV/H^+ for specimen #1; 0.65 keV/H^+ for #2; and 1.5 keV/H^+ for #3. Following H_3^+ irradiation, the specimens were thermally desorbed in vacuum, with a temperature ramping rate 2.5 K/s, to 1070 K, held for 4 min, and then cooled down with a cooling rate of 1 K/s. The purpose of the thermal desorption stage was to determine whether the release of hydrogen after bombardment would alter the optical properties of the mirrors. Comparison of reflectance measured by ellipsometry for the heated and unheated specimens indicated no effects due to post-irradiation heating [5]. Following the heating stage, all specimens were cleaned using an electron cyclotron (frequency $f = 2.375$ GHz) plasma discharge in D_2 in a simple double magnetic mirror device [7] for 15 min ($E_i = 50–65$ eV, $I_i = 16$ A/m^2). This soft cleaning is routinely used in our simulation experiments for organic contamination removal.

Several surface analysis techniques were used to study the hydrogen ion bombarded SS mirror surfaces. Micrographs were taken of the surfaces of all specimens using an optical microscope and interferometer (reflected regime) with magnifications of 100× and 400×, respectively. Scanning electron microscopy (SEM) was also used to study the surface topography.

A twin-wave interferometer was used to investigate the surface structure after ion bombardment. The interferogram, a set of light and dark stripes, is a result of the interaction of two coherent light beams reflected from the specimen and from a standard mirror. If the surface is ideally flat, these stripes on the interferogram will be parallel; otherwise, the stripes will distort and shift over irregularities (e.g., convexities, concavities, steps) of the surface under study. By measuring the shift ΔA, the depth (or height) h of such irregularities can be obtained from:

$$h = \frac{\lambda}{2}\frac{\Delta A}{A}, \tag{1}$$

where A is the distance between undistorted stripes and λ is the wavelength of light.

The optical characteristics of the specimen surfaces were also investigated by ellipsometry at a fixed wavelength (632.8 nm) and modeled as a homogeneous thin layer on a SS substrate using the technique applied in [5,8]. Ellipsometry measures the ratio $\rho = r_P/r_S$ of parallel (P) to perpendicular (S) reflectance coefficients of a specimen. The measured complex ratio ρ_{exp} is usually expressed in terms of measured ellipsometric parameters, i.e., the angles Ψ and Δ, where $\tan\Psi$ corresponds to the relative attenuation and Δ to the phase shift

between the P and S components of the reflectance coefficients [8]. The thickness of this layer and its optical indices were obtained from the ellipsometric data. Then, using the optical indices for the modified layer and indices measured for a virgin SS surface, the reflectance R at normal incidence was estimated according to [9]. The ellipsometric measurements were taken at different angles of incidence from 50° to 70° at room temperature with the null – LEF-3M-1 laser ellipsometer, described in detail elsewhere [10]. Four-zone averaging was used to reduce errors to about $\leqslant \pm 0.04°$ for Ψ and $\leqslant \pm 0.06°$ for Δ in measuring ellipsometric characteristics. These results were used to determine optical constants of the specimen and to model its surface layer.

Optical microscopy, interferometry, SEM, and ellipsometry are based on different physical mechanisms and complement each other in surface analysis.

3. Optical microscopy and interferometry data

The changes to the surface micro-relief after ion impact were analyzed by optical microscopy and interferometry as function of the ion beam energy. Fig. 1(a), (c) and (d) present optical microscopy viewgraphs of specimens #1, #2, and #3, respectively, following H^+ ion bombardment. The main effect of H^+ ion bombardment is connected with the sputtering erosion of the mirror material. The first indication that something different occurs in SS during H^+ bombardment was the appearance of the surface topography for specimen #1 (0.3 keV/H^+) in Fig. 1(a); optical contrast is indicated by arrows in the bombardment region. However, there is no visible boundary between the bombarded and virgin regions in this case. The interferogram of specimen #1, shown in Fig. 1(b), consists of parallel stripes which show very little distortion (indicated by white arrows) across the grain boundaries. The maximum difference between the levels of different grain surfaces is ~0.03 μm. This implies that the level (height or depth) of the bombarded region has to differ from the virgin surface by not less than ~ 0.03 μm. The double arrows in this figure indicate the zero-order interference stripe.

For specimens #2 (Fig. 1(c)) and #3 (Fig. 1(d)) the beam spot (region II) is clearly distinguished from the unexposed regions on the specimen (region I), and a sharp boundary is observed between the regions; see bold black arrows in Fig. 1(c) and (d). Note that the contrast increases with increasing energy. For specimens #2 (0.65 keV/H^+) and #3 (1.5 keV/H^+) mosaic relief has

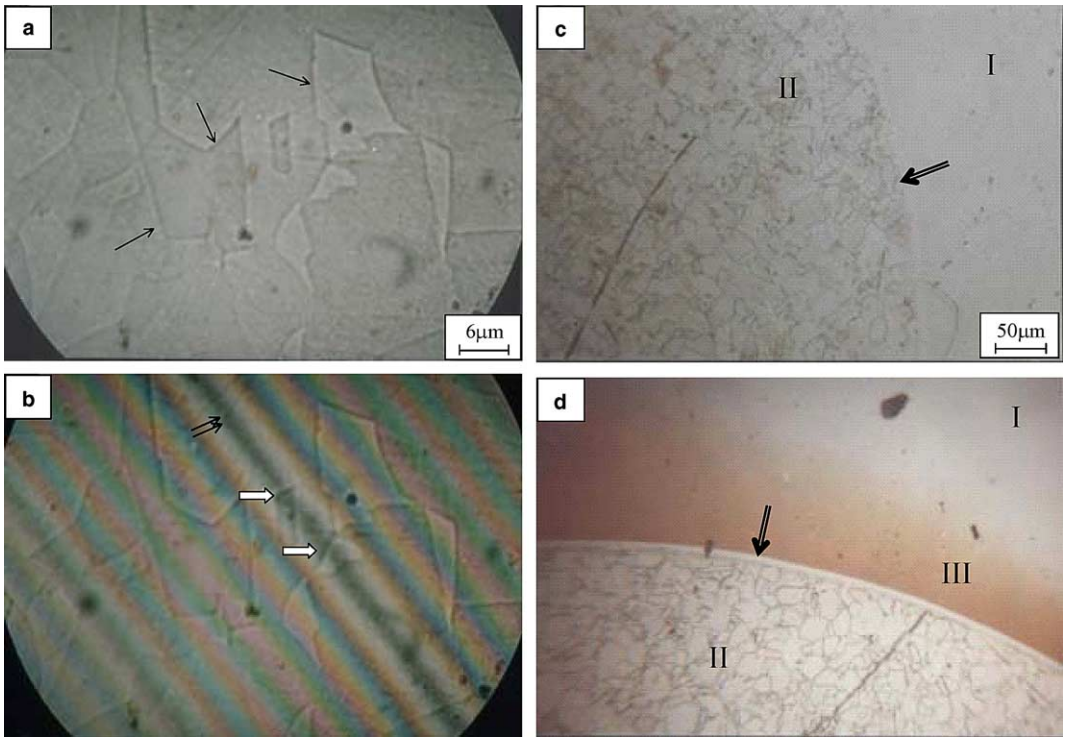

Fig. 1. Optical microscopy photographs of the surfaces of the SS mirror specimens: (a) #1; (c) #2; and (d) #3. The black arrows in (a) point to grain boundaries and the black arrows in (c) and (d) point to the beam spot edge. Interferometry microphotographs for specimen #1 are shown in (b) where the double arrows indicate the zero-order interference stripes.

developed inside the beam spot. It is evident from these photographs that the beam spot becomes identifiable due to some fundamental change in the near-surface morphology or surface topography under hydrogen ion irradiation. There is also a region of noticeable contrast surrounding the beam spot, (zone III in Fig. 1(d)), which appears only on specimen #3 (1.5 keV/H^+). This may be related to the deposition of sputtered material behind the edge of the mask covering part of the specimen during irradiation. The most striking observations in Fig. 1(c) and (d) are the color differences of regions I and II, and the development of region III. It appears that the surface topography has developed evenly over surface features and grain boundaries after irradiation. The main effect of increasing the H^+ ion energy is the appearance of a larger and somewhat better defined grain structure on the beam spot. The mosaic relief in the bombarded area is very similar to that which grows due to selective etching of crystal grain boundaries and reflects the morphology of the SS polycrystalline structure [11].

Fig. 2 shows optical microscopy photographs of specimens #2 (Fig 2(a)) and #3 (Fig. 2(c)). The boundary between the virgin surface and the beam spot (bold black arrows) can be clearly seen in the figures. Fig. 2(b) and (d) show interferometry pictures of the same regions for both specimens, respectively. A smooth knee is observed in the interference stripes over the edge of the beam spot, indicated by bold black arrows in Fig. 2(b) and (d). This knee is a result of the bombarded surface being lower relative to the virgin surface and is caused by the mass loss due to sputtering. The dependence of the beam spot depth near its edge derived from the interferograms versus ion energy is shown in Fig. 3. The data are seen to correlate well with the energy dependence of the sputtering yield, Y [12].

At points within the beam spot, the interference stripes also make sharp deviations; see white arrows in Fig. 2(b) and (d). This observation indicates that steep steps have formed at grain boundaries. It is possible to measure stripe shifts, using a white light source. Stripe shifts were determined using the zero-order stripes indicated with double black arrows in Fig. 2(b) and (d). The step heights and erosion depths were determined by Eq. (1) and were found to increase with H^+ energy; see Table 1. The height on the grain boundaries varies from $\sim$0.03 μm (0.3 keV/H^+) up to $\sim$ 0.23 μm (1.5 keV/H^+).

In brief, SS bombardment by hydrogen ions results in the formation of an eroded region with well-defined

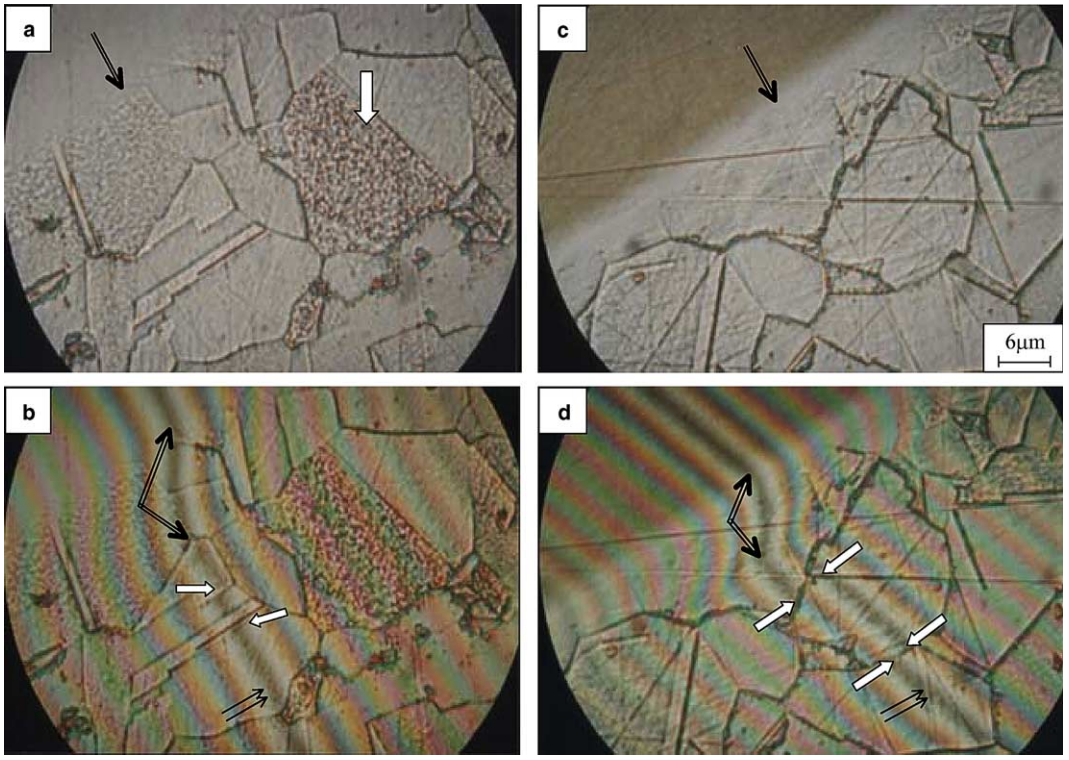

Fig. 2. Optical microscopy photographs of specimens #2 and #3 in (a) and (c), respectively; the boundary between the virgin surface and the beam spot (black arrows) can be clearly seen. The interferometry microphotographs in (b) specimen #2, and (d) specimen #3, coincide with the regions shown in (a) and (c), respectively. The double black arrows in (b) and (d) indicate the zero-order interference stripe.

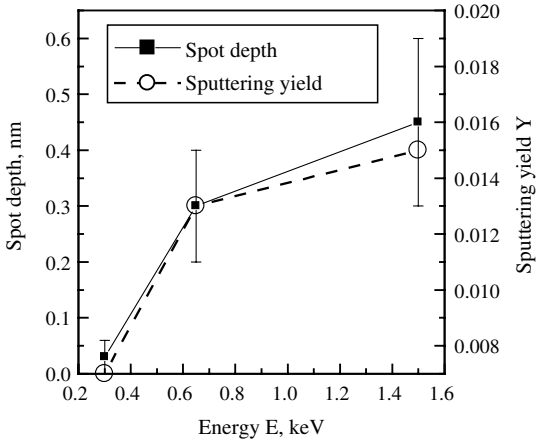

Fig. 3. H^+ ion energy dependence of the beam spot depth near its edge derived from the interferograms (from Table 1). For comparison, the H^+ energy dependence of the sputtering yield, Y, is also plotted [12].

Table 1
Beam spot depths and step heights at grain boundaries of specimens #1, #2, and #3

	Specimen (H^+ energy)		
	#1 (0.3 keV)	#2 (0.65 keV)	#3 (1.5 keV)
Spot depth (μm)	0.03 ± 0.03	0.3 ± 0.1	0.45 ± 0.15
Step height at grain boundaries (μm)	0.03 ± 0.03	0.12 ± 0.03	0.23 ± 0.13

mosaic relief, which can be distinguished using a microscope by color and contrast. The step structure observed is typical for polycrystalline materials under ion irradiation [7,11]. Its appearance is explained by differences in sputtering yields for grains with different orientations. The step height increases with increasing ion energy. The development of surface topography during sputtering also consists of some in-grain surface roughening, as evidenced by the fuzziness of some interference stripes in Fig. 2(b) and (d).

The optical microscopy and interferometry study of the SS surface is used for the development of a physical model of the damaged layer formed as a result of hydrogen ion irradiation. The beam spot consists of crystals (grains) with different orientation and grain boundaries. Parameters of the model (namely, optical constants and thickness of the damaged layer) can be determined from ellipsometric experimental results, as discussed below.

4. Ellipsometric data and physical model of damaged surface layer

Ellipsometry is one of several nondestructive techniques used to study damaged surface layers created after low energy ion bombardment. Since ellipsometry uses light that penetrates the SS surface to tens of nanometers, it is sensitive to surface variations caused by hydrogen ions, which penetrate ~10 nm into SS at ~1 keV/H^+ [13].

The technique has been discussed elsewhere [10,14]. Here we use the ellipsometric data obtained in this study for the assessment of plausible physical models of the damaged surface layer formed during H^+ irradiation. Several models for the analysis of the ellipsometric data were treated. As a first step, the data were analyzed assuming only the bulk substrate (specimen – air), giving the so-called apparent optical constants. This model is adequate for the unirradiated virgin region of the specimen.

However, for the irradiated beam spot, one would expect that the optical constants would be affected by the erosion roughness of the specimen. Although, for the specimens studied here, the lateral dimensions and relative heights of the grains were 30–50 μm (Fig. 2) and ~ 0.2 μm (Table 1), respectively, according to [15], it is not necessary to take this roughness into account. Thus, a model of one homogeneous isotropic layer on a homogeneous isotropic substrate was assumed. This single homogeneous damaged layer model is sufficient in the absorptive spectral region for our photon energy, when the contribution of the substrate cannot be neglected. We tried to confirm this in the following way.

From the measured optical constants the penetration depth D of the light can be computed readily (as a first step). This is the inverse of the absorption coefficient K_S, which is proportional to the imaginary part of the complex refractive index:

$$N_s = n_s + ik_s, \quad K_s = 4\pi\nu k_s, \quad D = 1/K_s, \tag{2}$$

where ν is the wave number ($\nu = 8066E$ when ν is in cm^{-1} and the photon energy E is in eV). The field amplitude is attenuated by a factor of $\exp(-K_S x/2)$ when passing a layer of thickness x. This means that a film thickness larger than $\sim 2D$ makes the substrate practically invisible in the reflected light, since the corresponding attenuation factor $\exp(-4)$ of the forward and backward passes of light is less than 0.02. The penetration depth of the incident light computed from the measured ellipsometric data according to Eq. (1) is ~ 15 nm. So, the damaged layer (~ 10 nm [13]) caused by H^+ irradiation is half-transparent. Thus, it is obvious that while modeling this layer one cannot neglect the influence of the substrate on reflectance, i.e., the polarization properties of the probing light contain information not only on the light interacting with the damaged layer but with the substrate as well.

Ellipsometric angles Ψ and Δ for the substrates (virgin surface) and for the beam spots of the three specimens (#1, #2, #3) were measured. The optical constants of the specimen substrates were determined from the

data obtained at several locations on the specimens (unexposed to H^+ ions) and then averaged prior to the analysis of the beam spot. It is assumed that the main strain layer originating from mechanical polishing (with $n_S = 2.32$; $k_S = 3.65$ [5]) was modified by the post-irradiation heating to 1070 K in vacuum, i.e., the heating procedure has led to a reduction in the measured optical parameters n_S and k_S. For the analysis that follows, it is assumed throughout that this is a reasonable first approximation for the heat-modified SS substrate. Processing of the ellipsometric data for this heat-modified virgin surface gave the following optical indices: $n_S = 1.81$; $k_S = 3.51$; see Table 2. The normal reflection coefficient R calculated using these data according to [9], is 64% and corresponds to results of previous experiments with SS mirrors [5].

Fig. 4 shows the dependence of the ellipsometric angle difference $\delta\Delta$ between the virgin surface (Δ_S) and the beam spot (Δ_B) upon the incidence angle θ for specimens #1, #2 and #3. Significant changes in the optical properties of SS mirrors under bombardment were revealed.

Table 2
Physical parameters of the SS damaged layer for specimens #1, #2, #3

Specimen	E (keV/H^+)	SS damaged layer parameters			R (%)
		n_L	k_L	d_L (nm)	
#1	0.3	1.35	2.79	4.0	64
#2	0.65	1.62	2.97	9.0	63
#3	1.5	1.75	3.01	12.6	62

Substrate optical parameters: $n_S = 1.81$, $k_S = 3.51$, $R_S = 64\%$.

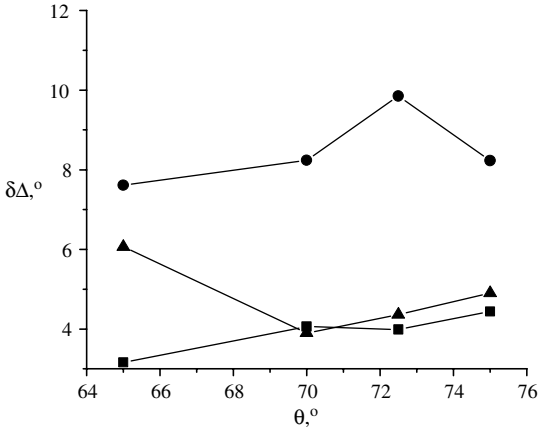

Fig. 4. Dependence of $\delta\Delta$ on the incidence angle θ for specimens #1 (■), #2 (▲) and #3 (●), where $\delta\Delta$ is the difference of ellipsometric angles for the heat-modified virgin surface (Δ_S) and the beam spot (Δ_B).

So, ellipsometry was found to be sufficiently sensitive to detect surface modifications created by H^+ irradiation.

To calculate n_L and k_L for the beam-damaged layer from the ellipsometric angles it is necessary to develop a physical model of the surface layer after H^+ irradiation. Processing of the ellipsometric data for the beam spots was carried out using several models based on physical considerations relating to the peculiarities of the interaction of the hydrogen ion beam with the SS surface at various energies. The choice of an adequate model was based on our optical microscopy and interferometry results. The optical microphotographs gave reason to model the damaged layer on the specimens with a conventional homogeneous film.

Table 2 shows the physical model applied to all three specimens. Varying the energy has resulted in a change of the refraction and absorption indices, but without noticeable change of the calculated reflectance at normal incidence R. This result is in agreement with the experimental data for R reported in [11]. The optical parameters n_L and k_L for the beam-damaged layer are also plotted as a function of H^+ energy in Fig. 5. The main variation of these indices takes place for H^+ energies below $\sim$0.65 keV/H^+. The change of these indices between 0.65 and 1.5 keV/H^+ is relatively small.

Using the latest version of TRIM, SRIM2000 [16], ion range calculations were performed for H^+ impact on SS for the three energies used in the experiment. The mean penetration depth is shown in Fig. 6; the shaded region represents one standard deviation about the mean value. The experimental values for the damaged layer thickness, d_L, (from Table 2) are also shown, and for the ion fluence used in the present experiment they all fall inside this shaded zone. This relatively good agreement supports the reliability of the optical constants n_L and k_L obtained in our experiments for the damaged SS layer and the adequacy of the models.

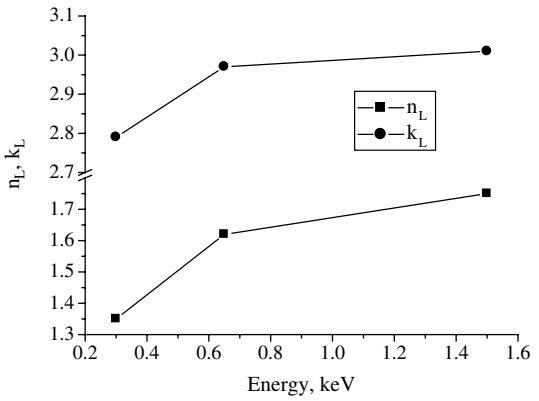

Fig. 5. Dependence of optical parameters n_L and k_L for the beam-induced damaged layer on H^+ energy.

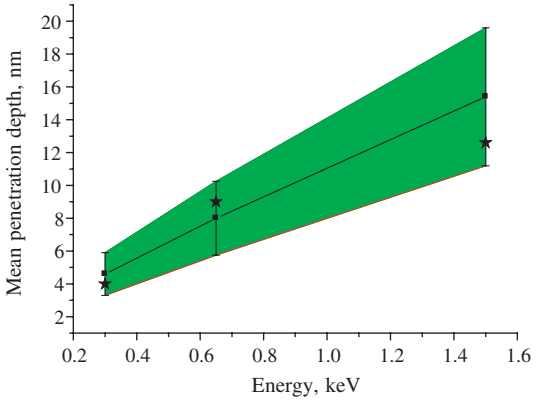

Fig. 6. Dependence of mean penetration depth on H^+ energy as calculated by TRIM (SRIM2000) [16]. The solid line and solid squares are the calculated values; the shaded region represents one standard deviation about the mean value. The values of the damaged layer thickness, d_L, (Table 2) derived from the model are shown by the star symbol.

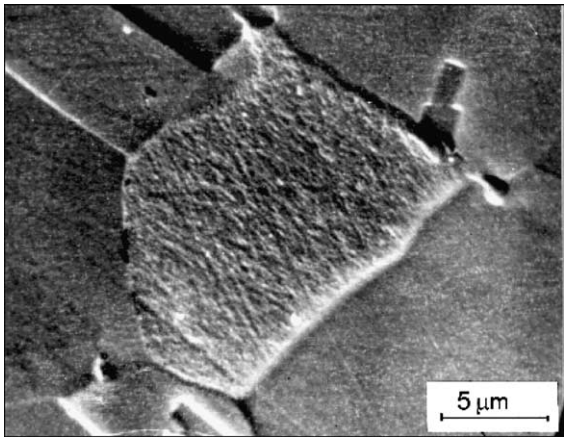

Fig. 7. The SEM microphotograph clearly reveals the surface roughening on one of the grain surfaces on the beam spot of specimen #3.

5. Discussion

The model of the damaged surface layer on SS (see parameters in Table 2) and the process of modified layer formation as a result of H^+ irradiation were proposed on the basis of the experimental data. The main steps involved in surface modification and the general picture after sputtering by H^+ (1.5 keV/H^+) are as follows. The initial 'hard' surface (produced during the polishing process, with $n_S = 2.32$ and $k_S = 3.65$ [5]) has been altered by post-irradiation heating in vacuum. The surface became 'softer' ($n_S = 1.81$; $k_S = 3.51$) after removing the strained layer with increased density of defects and stresses.

The bombardment by hydrogen ions with 0.3 keV/H^+ energy and a fluence $\sim 2 \times 10^{24}$ H^+/m^2 only partially removes this strained layer. Traces of this kind of layer still appear to exist on the specimen surface exposed to 0.65 keV/H^+ ions, as indicated by the white arrow in Fig. 2(a). However, at 1.5 keV/H^+ energy the strained layer obscuring the substrate signal has almost completely been removed (Fig. 2(c)). In this case all grains appear to have only one color.

It is observed that a larger and somewhat better defined grain structure appears in the beam spot as the H^+ ion energy increases. Optical microscopy shows that with 1.5 keV/H^+ ions the surface topography, i.e., the step structure, develops rather evenly over the surface and grain boundaries. However, surface roughening inside some grains can also be found. For one of these grains, the surface roughening clearly seen on a SEM photograph (Fig. 7) is much stronger in comparison with the other nearby grains (similar to [6]). It is not clear why the surface roughness is not observed for all crystallographic planes and why no direct correlation was found between sputtering yield and the in-grain roughness [6]. Perhaps it is due to the fact that grains with different orientations in polycrystalline materials are characterized by different defects and energy, leading to fundamental differences in sputtering (etching) processes. The most closely packed planes, e.g., (1 1 1)-type, look smooth on SEM photographs [6]. Other inclined planes show defects and structure imperfections in the sputtering process, possibly causing the experimentally observed roughness relief.

It is evident from the experimental results that the development of surface topography during the sputtering process consists of surface roughening along with some enhancement of grain structure relief. The fact that the optical parameters n_L and k_L are relatively constant for the 0.65 and 1.5 keV/H^+ energies (Fig.5) indicates that no significant variation in the optical characteristics of the surface across the specimen occurs during irradiation at these energies. This is in approximate quantitative correspondence with the small sputtering yield difference for H^+ ions with 0.65 and 1.5 keV/H^+ energies in comparison to the yield difference for 0.3 and 0.65 keV/H^+ (Fig. 3).

It should be noted that in the present study the observed behavior of the grain structure is definitely the result of sputtering – not the result of post-irradiation heating – because similar structures were observed for SS specimens which have not been heated in vacuum after hydrogen ion irradiation [5].

6. Conclusions

The bombardment of stainless steel mirrors with hydrogen ions leads to changes in the morphology and structure of a stainless steel surface. In principle, there

are two different processes on a SS surface subjected to sputtering by hydrogen ions: (i) strained surface layer removal and (ii) the formation of a step structure in the bulk (i.e., not strained) SS material.

The damaged surface layer formed on the SS mirror specimens during ion irradiation can be reliably modeled with a homogeneous layer which is less dense than the virgin material for energies of up to 1.5 keV/H^+. The optical constants n_L and k_L of this layer vary with energy, but without noticeable variation of reflectance at normal incidence, R. These measurements confirm that a large factor in the loss of reflectivity experienced by SS mirrors under H^+ bombardment [5] is the differing erosion of individual grains. In agreement with the results of [17], we conclude that such mirrors would be more resistant to losses in reflectivity were they made from single crystals instead of polycrystalline steel. Further studies of the type carried out by Balden et al. [6] will be required to clarify the issue of which crystal orientations provide the best response to H bombardment in fusion devices.

The results obtained demonstrate the capabilities of optical microscopy, interferometry, scanning electron microscopy and ellipsometry to perform detailed investigations of microstructure and topography of SS mirror specimens subjected to long-term H^+ irradiation. In particular, ellipsometry is a very useful non-destructive technique for investigating the effects of nm scale non-homogeneous layers on solid surfaces.

Acknowledgement

We (the University of Toronto coauthors) gratefully acknowledge the funding provided by the Natural Sciences and Engineering Research Council of Canada.

References

[1] R.M. Giannella, CEA Cadarache, Private communication.
[2] M. Lipa, B.Schunke, Ch. Gil, V.S. Voitsenia, V. Konovalov, K. Vukolov, M. Balden, G. De Temmerman, P. Oelhafen, A. Litnovsky, P. Wienhold, Analyses of metallic first mirror samples after long term plasma exposure in Tore Supra, in: Accepted for Presentation at the Seventh International Symposium on Fusion Nuclear Technology (ISFNT-7), 22–27 May 2005, Tokyo, Japan.
[3] V.S. Voitsenya, A. Sagara, A.I. Belyaeva, V.N. Bondarenko, A.D. Kudlenko, V.G. Konovalov, S.I. Solodovchenko, Plasma Devices Oper., accepted for publication.
[4] K.Yu. Vukolov, M.I. Guseva, S.A. Evstigneev, A.A. Medvedev, S.N. Zvonkov, Plasma Devices Oper. 12 (2004) 193.
[5] A.F. Bardamid, A.I. Belyaeva, V.N. Bondarenko, J.W. Davis, A.A. Galuza, I.E. Garkusha, A.A. Haasz, V.G. Konovalov, A.D. Kudlenko, M. Poon, I.V. Ryzhkov, S.I. Solodovchenko, A.F. Shtan, V.S. Voitsenya, K.I. Yakimov, Phys. Scr. T103 (2003) 109.
[6] M. Balden, A.F. Bardamid, A.I. Belyaeva, K.A. Slatin, J.W. Davis, A.A. Haasz, V.G. Konovalov, M. Poon, A.N. Shapoval, V.S. Voitsenya, J. Nucl. Mater. 329–333 (2004) 1515.
[7] A. Bardamid, V.T. Gritsyna, V.G. Konovalov, et al., Surf. Coat. Technol. 103&104 (1998) 365.
[8] A.I. Belyaeva, A.A. Galuza, Physica B 304 (2001) 333.
[9] G. Hass, J. Opt. Soc. Am. 47 (1957) 1070.
[10] A.I. Belyaeva, A.A. Galuza, T.G. Grebennik, V.P. Yuriev, Adv. Cryogen. Engin. (Materials) 46 A (2000) 435.
[11] A. Bardamid, V. Bryk, V. Konovalov, et al., Vacuum 58 (2000) 10.
[12] Y. Yamamura, H. Tawara, Atom. Data Nucl. Data 62 (1996) 149.
[13] B. Sherzer, in: R. Behrisch (Ed.), Sputtering by Particle Bombardment, Springer, Berlin–Heidelberg–New York–Tokyo, 1983.
[14] R.M.A. Azzam, N.M. Bashara, Ellipsometry and Polarized Light, North-Holland, Amsterdam, 1977.
[15] D. Franta, I. Ohlidal, Mod. Optic. 45 (1998) 903.
[16] J.F. Ziegler, J.P. Biersack, TRIM 2000, SRIM version 2000.40.
[17] V. Voitsenya, A.E. Costley, V. Bandourko, et al., Rev. Sci. Instrum. 72 (2001) 475.